Towards Cooperative Grids: Sensor/Actuator Networks for Renewables Integration

Jay Taneja, David Culler
Computer Science Division
University of California, Berkeley
Berkeley, California 94720
Email: taneja,culler@cs.berkeley.edu

Prabal Dutta
Computer Science Department
University of Michigan, Ann Arbor
Ann Arbor, Michigan 48109
Email: prabal@eecs.umich.edu

***Abstract*—Faced with an uncertain path forward to renewables portfolio standard (RPS) goals and the high cost of energy storage, we believe that deep demand side management must be a central strategy to achieve widespread penetration of renewable energy sources. We examine the variability of wind as a source of renewable, non-dispatchable energy and the loads that can be dispatched to match sources of this type. We identify two classes of dispatchable energy loads, and create models for these loads to match their consumption to the generation of energy sources, while introducing *slack*, a generalized measure of dispatchability of energy. From these load models, we examine a number of techniques and considerations for source-following loads, including the sensitivity of thermostat constraints and the effects of aggregating appliance populations. Our results show a home heater that is able to reduce energy consumption by over 50% while increasing the proportion of renewable energy consumed versus grid energy.**

I. Introduction and Background

A regulatory push for renewables to play a larger role in the mix of energy sources is well underway in many states across the U.S. Already, 36 of the 50 states have set goals for a Renewables Portfolio Standard (RPS) of anywhere from 10 to 25% of total energy consumed [1] and California has called for renewables to comprise 33% of its energy mix by 2020 [2]. However, as the fraction of energy from renewable, but non-dispatchable, sources like wind and solar increases, it will become more difficult to match supply and demand because today's loads are largely oblivious to supply variations.

Beyond existing demand response programs [3], we propose *deep demand response* – a distributed conjoining of energy information with physical control systems enabled by pervasive sensor/actuator networks – to dynamically match supply and demand down to the appliance-level. The two keys to matching supply and demand in real-time are predicting the output of renewable sources and controlling the consumption of loads in response to these dynamic predictions. The challenge lies in meeting the quality-of-service requirements of the load while adapting to variations in the source. To model source variability, we consider the cumulative distribution function (CDF) of the source *ramp rate*, or change in output. To reason about load adaptability, we use the notion of energy *slack*. Intuitively, slack refers to the amount of time an energy-consuming operation can be advanced or delayed.

To make our proposal more concrete, consider the example of wind as the renewable source and the refrigerator as a programmable load. Figure 1 shows the variability of a wind source over different time frames using a year of data. For example, the output power changes by less than 5 kW over a 5 min window 95% of the time, but up to 25 kW over a 60 min window 95% of the time. Now, imagine

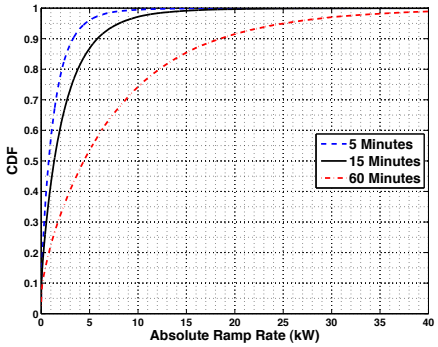

Fig. 1. Wind ramping. Although wind is unpredictable over longer times frames, like hours, its short-term variability, over tens of minutes, is quite predictable. This energy information can be used to dispatch loads and take advantage of slack, either by advancing or delaying energy consumption.

if this kind of energy information were available to loads (perhaps in aggregate). Then, intelligent, networked loads could adapt their behavior to be greedy or miserly with energy consumption. For example, a refrigerator could advance the start time of its cooling cycle to consume excess energy, or a temperature setpoint could be slightly increased to reduce energy consumption. In the first case, pre-cooling changes the phase of subsequent cooling cycles, while in the second case, changing the temperature setpoint (for a cycle or two) reduces the energy consumption.

II. Energy Sinks

In order to make reasoned decisions in sculpting energy loads, it is important to have a metric to express *how sculptable* a load is, both in magnitude as well as time. Without a way to quantify whether energy should be consumed now or later, control decisions cannot be made optimally. Further, in order for a load to be sculptable, we argue that (1) its consumption schedule involves choices on when to consume energy and (2) there is either some capacity to store energy in the system OR there is "slide" in the task the device is to complete. Slide, the ability to schedule consumption, is prevalent in those operations when quality-of-service is defined by the user. Table I presents a number of devices that are capable of sculptability, along with their energy storage type and an estimate of their control schedule.

The ability to manipulate dispatchable loads enables a controller to improve the alignment of energy supply and consumption. However, the rapidly changing availability of energy supply and the consumption of non-dispatchable loads dictates that the controller must make decisions continually.

Device	Control Schedule	Energy Storage	Time Horizon (min/max)
Thermostatically Controlled			
Refrigerator/Freezer	Range maintenance, bang-bang or variable drive	Thermal storage	5m/1h
Building Heating, Ventilation, and Air Conditioning (HVAC)	Range maintenance, bang-bang or variable drive	Thermal storage	5m/1h
Chiller	Range maintenance, bang-bang or variable drive	Thermal storage	5m/1h
Water Heater	Range maintenance, bang-bang	Thermal storage	5m/1h
Slide			
Washing Machine	On-demand with optional slide	Slide	1m/30m
Clothes Dryer	On-demand with optional slide	Slide	1m/1h+
Batch Computing	On-demand with optional slide	Slide	1m/8h+
Dishwasher	On-demand with optional slide	Slide	1m/8h
Coffee Maker	Range maintenance, bang-bang	Slide	1m/30m
Plug-in Vehicle	Range maintenance, bang-bang	Electrochemical storage	1m/8h

TABLE I
COMMON ENERGY LOADS THAT ARE AMENABLE TO SCULPTING.

Though, in order to better schedule energy consumption, we need not only information on flexibility of load schedules, but also estimates on the magnitude of energy available for scheduling. This calculation is trivial for job-based operations that have well-understood consumption such as clothes washing and drying machine loads, but not as clear for systems that attempt to maintain certain conditions through negative reinforcement feedback such as heaters, air conditioners, and refrigerators. To generalize the concept of energy available for dispatch, we introduce a metric called *slack* and continue by modeling a set of common dispatchable loads.

A. Slack

To represent the range of dispatchability opportunities – varying from low- to high-power loads, short- to long-running operations, and one-time to continuous tasks – we introduce the notion of *slack*, or the potential of an energy load to be advanced or deferred without affecting earlier or later operations or outcomes. In critical path analysis, slack refers to the scheduling flexibility in a non-critical path task that keeps the task off the critical path. Slack is a basic and well-understood concept in many disciplines, but in this instance, we measure it in common units of energy and apply it to the operation of physical systems, where the goal is not completion time. Usually, in physical systems, we are concerned with some other input and output variables – in the case of a kitchen fridge, we might ask: *How sculptable is the refrigerator load?*

More important is the question of how much can we shift the refrigerator's compressor cycle (and the resulting power draw) while keeping the temperature within an acceptable operating envelope. To make the discussion more concrete, consider Figure 2(a), which shows one fridge operating cycle consisting of forced cooling (from time t_0 = 00:00 to time t_1 = 00:11) and natural warming (from time t_1 to time t_2 = 00:59). The lower temperature threshold, T_ℓ, is at 2.6°C and the upper threshold, T_u, is at 3.4°C. The corresponding power consumption of the fridge is shown in Figure 2(b).

At time t_0, the beginning of the forced cooling cycle, the slack s_w begins at 0. In other words, we can not postpone the forced cooling phase any more, as the temperature has risen to cross the upper threshold T_u. Indeed, this is precisely the control law that a refrigerator follows today. As the time progresses from t_0 to t_1, the energy slack s_c increases according to the accumulation of the energy input $E(t)$ into the system as a function of the system power $P(t)$; in this case this is the power consumption of the compressor.

$$s_c(t_c) = E(t) = \int_{t_0}^{t_c} P(t)\,dt$$

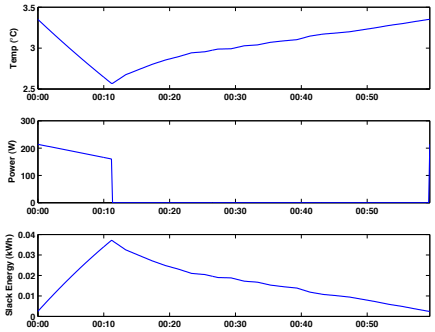

Fig. 2. The operating cycle of a fridge: (a) temperature, (b) power consumption , and (c) energy slack.

For simplicity, we assume that the conversion of electrical energy to cooling energy by the compressor is perfect – though not true, we believe it is unnecessary to differentiate between slack energy and energy input for this process.

Now let us consider the slack during the natural warming phase. Initially, the slack is at its peak value for this cycle, as the cooling phase has just ended and the temperature has dropped to its lower threshold T_ℓ. As the warming phase starts, the temperature begins to rise and the slack energy stored in the system degrades. To determine the slack during the warming phase, we must find the slack during the cooling phase with the corresponding temperature in the warming phase. Let $T_w(t)$ be the temperature during the warming phase at time t, where $t_1 \le t \le t_2$ and let $t_c(T)$ to be the time during the cooling phase as a function of the temperature T. Recall that the slack in the cooling phase is $s_c(t) = \int_{t_0}^{t} P(t)\,dt$. We can now substitute $t_c(T_w(t))$ for t, which gives the slack s_w during the warming phase as

$$s_w(t_w) = \int_{t_0}^{t_c(T_w(t))} P(t)\,dt$$

where $t_1 \le t \le t_2$.

Computing the slack using collected values for P(t) and T(t), we can calculate the slack energy as a function of time over a cycle of the refrigerator, as seen in Figure 2(c).

Assuming $t_w(T)$ and $T_c(t)$ are known or can be computed, we can plot slack as a function of time, as Figure 2(c) shows. More simplistically, energy slack closely follows a banking metaphor – as energy is used by the system to do work (in this case, operate the compressor), slack is accrued in the slack "account." Then, during the natural warming cycle, the account is drained and the slack is slowly reduced. Also, just as deposits remain in a bank account, slack remains in a system across cycles in the form of stored energy. In the case of

a battery, this is the capability to introduce energy into the system later. For a refrigerator, this is the thermal energy stored in the contents of the fridge, whether they are food, liquids, or even air (though these each have different capacities for energy storage, as discussed later in Section II-B).

B. Modeling Sinks

Having developed a metric for dispatchability, we now describe the creation of models of individual consumers of energy to compose an integrated model of energy loads found in a building. In this section, we examine thermostatically-controlled loads – namely, a refrigerator and a heater – as well as loads that have slide – a clothes washer, clothes dryer, and coffeemaker. These models can then be composed and sculpted in response to energy generation variations.

1) Thermostatically-Controlled Loads: A common class of energy loads seek to maintain the temperature of a medium within predetermined constraints. In most cases, this is done through closed-loop feedback, actuating when a temperature sensor detects that the lower or upper bound is reached. The medium under control varies – sometimes liquid (e.g. water in a water heater), solid (e.g. food in a refrigerator), or gas (e.g. air in a building) – as does the duty cycle of the actuation operation for maintaining the desired temperature range.

In this section, we demonstrate how to generate a model of an example thermostatically-controlled system, with the purpose of enabling accurate simulation of operation under different constraints. Using the empirical vehicle of a refrigerator, a characterization of the warming and cooling phases of the system is performed to generate a distribution of curves to be used in the model. Then, the curves are followed and actuation is performed according to preset control laws to simulate operating behavior of the system. We then show how this basic technique can be applied to another thermostatic system, the heating system in a house.

The experimental data gathered for this study was collected using a network of 4 Sensirion SHT15 temperature and relative humidity sensors coupled with a Hamamatsu S1087 photodiode and 1 wireless AC Electricity Meter. Three of the climate sensor suites are deployed inside the refrigerator, attached to the underside of different shelves, while the fourth climate sensor suite is attached to the outside of the fridge. The AC Electricity Meter is in series with the refrigerator/freezer power connection. The refrigerator used for the measurements is an 18 cu. ft. General Electric model GTS18FBSARWW. The climate sensor suites are sampled every 10 seconds, while the electricity sensor is sampled every second – this helps for capturing transient electrical loads due to compressor start-up.

Each sensor or sensor suite is attached to a low-power, wireless mote that is running an IPv6-compatible networking layer. The motes form an ad-hoc network along with a laptop that acts as both an edge router for Internet access and a data storage entity, recording data samples into a MySQL database. Having all of the sensors on a network was important for correlating events between sensors as well as automating the gathering of sensor data.

The fridge was monitored for over 3 months at various set points, though only six days of data from one sensor suite and one electricity meter, all at the same set point, were necessary for this study. Over the six days, each cycle of the refrigerator was identified by observing electricity consumption – if the fridge was consuming electricity, it was in the cooling phase, otherwise it was in the warming phase. Over six days, this identified a total of 153 cycles, or just over one cycle per hour. Then, data from the photodiode were used to identify and remove any cycles that may have been perturbed by a door opening event, as this fridge is in regular use.

To model the warming phase of the temperature curve, a number of different techniques were used. Looking at Figure 2(a), the curve resembles a decaying exponential approaching an asymptote. Physically, this squares with the intuition that the air temperature in the refrigerator asymptotically approaches the outside air temperature. The rate that this occurs is governed by the constant resistance of the fridge walls to conducting heat as well as the diminishing temperature difference between the inside and outside air. Consequently, the air temperature in the refrigerator increases, but the increase is delayed by convection of heat from the air to the food with its associated large thermal mass. In theory, modeling this temperature response calls for a regression using two exponential terms. In practice, however, the portion of the curve captured (roughly between 2.5 and 3.5°C) is a small portion of the entire warming curve, which would approach an outside air temperature of approximately 19-21°C. Thus, with a limited set of points, curve fitting solutions that minimize mean-squared error generally do not capture the shape of the curve in the limited domain, resulting in fits that are essentially linear over the domain under consideration. Thus, in order to accurately fit the warming curves empirically observed, we use a linear spline model that interpolates between the observed values and extrapolates to a wider domain by extending lines at the same slope as the end of the observed domain. We believe that the high rate of change of the temperature early in the warming phase is as a result of the low heat capacity of the air inside the fridge, which changes its temperature quickly. Once convective heat exchange between food and air becomes large, the fridge temperature change transitions towards being linear, and this pattern continues outside the measured domain. Thus, our linear spline extrapolation fits the behavior of the warming curves accurately for both the measured domain as well as the extended domain.

For modeling the cooling phase of the temperature curve, the factors contributing to the warming curve remain relevant. However, another component, the forced cooling action of the refrigerator compressor, not only counteracts the warming, but also cools the fridge at a significantly faster rate. This is evident in the durations of the cooling phase and warming phase – 12.3 minutes and 45.3 minutes over the 98 unperturbed curves, respectively. Thus, the extra power of the compressor allows the fridge to cool nearly four times as fast as it naturally warms. In practice, this diminishes the effects of the natural warming components in designing a model of the

cooling phase of the fridge. In addition, the power consumed also follows an exponentially diminishing curve during each cooling phase. For both, we use a simple exponential decay model with three parameters, according to the equation

$$T(t) = a_1 - a_2 * (1 - e^{(a_3 * -t)})$$

For each run of the fridge simulation, a set consisting of a warming, cooling, and energy curve is selected. These curves are not chosen independently because the shape and cooling rate of the cooling curve is dependent on the warming curve it follows, and the warming curves exhibit significant variations over the six days of data. The same holds true for the energy curve – its shape is linked to its corresponding cooling curve. In order to select a set of curves, we create a distribution of the curves using the average warming rate ($\frac{T_{end}-T_{begin}}{t_{end}-t_{begin}}$).

To run a simulation of the refrigerator, an initial condition is randomly chosen from the range of temperatures within the constraints of the operating range (known as the guardband), and an initial state (warming or cooling) is chosen according to the proportion of time spent in each phase (≈20% cooling, ≈80% warming). From there, temperature curves can be plotted according to the phase of the operating cycle. Additionally, values for the power curve can also be plotted concurrently. Whenever the simulated fridge reaches a guardband boundary, the phase is changed and a different curve is used. This simple fridge model, oblivious to its energy input and any other external signals, aims to recreate the behavior of an unperturbed fridge. Without variations in the guardband and no perturbation, the fridge merely repeats the temperature and power cycles seen in Figure 2, resulting in a compressor duty cycle of 19.0% with the set of curves selected, though the duty cycle varies between 13% and 35% for other curves.

Having modeled a specific thermostatic device, we would like to emphasize that the technique for constructing a model is generalizable to a wider set of energy loads. To this end, a data trace was collected for the temperature of a house. The house under observation resides in a relatively mild climate where outside air temperature is generally 5-10°C lower than the house temperature, and contains a heater but no air conditioner. In accordance with this temperature trace, a complementary electricity trace for a heater is synthesized. Note that the magnitude of power consumption is sized for only the fan of the furnace – gas heat is assumed. If an electric furnace was assumed, consumption would be significantly higher.

An important variation between the fridge and thermostat models created is that the fridge operating cycle is forced cooling and natural warming, while the thermostat is opposite – forced warming by the heater and natural cooling as the inside air approaches the temperature of the cooler outside air. Also, in this case, we do not create a distribution of curves, instead simply using a single warming and cooling curve as a proof-of-concept. The resulting trace of the temperature, power, and slack behavior of an oblivious thermostat over three hours is provided in Figure 3.

2) Slide Loads: The other class of dispatchable energy loads we examine in this work are those that can be scheduled

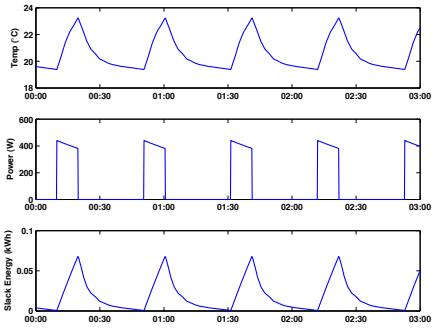

Fig. 3. The operating cycle of a house thermostat: (a) temperature, (b) power consumption , and (c) energy slack. The thermostat operates in a reverse pattern from the fridge, with an operating cycle that consists of forced heating followed by natural cooling. Thus, the energy slack is phase-shifted by 180 degrees from the refrigerator. The duty cycle of the heater is about 24.6%.

for completion in some timeframe. We expect that the flexibility of this type of load will depend highly on the quality-of-service demanded by the user; if people are not incentivized to be patient for completing their operations (i.e. if there is no preferable tariff or other benefit given for delaying the operation), then flexibility will be limited.

Examples of these loads are proposed in Table I; we recognize that typical appliances do not yet provide this capability. However, we believe that the emergence of plug-in electric vehicles – each of whose power consumption roughly equals that of an entire house, essentially requiring some sort of smart charging for a stable electricity grid – will make scheduled appliance operations more familiar to the general public.

Generating models for these appliances is straightforward: traces of example appliances were obtained from the Lawrence Berkeley National Labs Appliance Energy Use Data repository. [4] Each appliance was assigned an arrival pattern according to expected usage. Table II shows these arrival rates, and Figure 4 shows traces of a clothes washing machine, clothes drying machine, and coffeemaker. Note that the clothes dryer is in fact a gas model; using an all-electric clothes dryer would significantly increase electricity consumption.

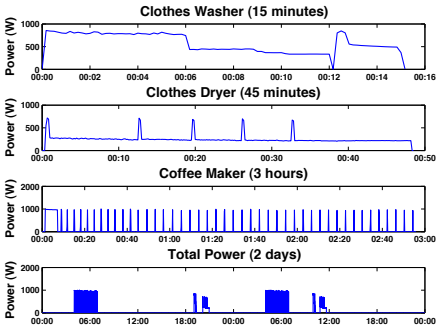

Fig. 4. Traces of power consumption of appliances listed in Table II. From these traces, a model over two days is created.

III. Integration Studies

In this section, we explore some of the implications of integrating groups of energy loads. As stated earlier, the primary purpose of exploring slack in energy loads is not for energy efficiency, but instead for advancing or deferring operations to better match energy consumption to generation.

Device Type	Model	Energy Per Operation	Arrival Schedule
Clothes Washer	Whirlpool Imperial	0.145 kWh	One load per day, starting randomly between 6 AM-9 PM
Clothes Dryer (Gas)	Whirlpool Imperial	0.199 kWh	One load per day, starting randomly within 1 hr. after washer completes
Coffeemaker	Cuisinart 12 Cup	0.249 kWh	Daily at 4 AM, remain warm until 7 AM

TABLE II
LOADS THAT HAVE SLIDE. EACH HAS BEEN MODELED FROM EMPIRICAL DATA; JOB SCHEDULING IS ASSUMED FOR A FAMILY OF FOUR.

However, flexibility (and thus, slack) is also improved by softening guardband constraints. Figure 5 shows the effect on the heater average power consumption from its baseline at 266.2 Watts by altering the guardband constraints.

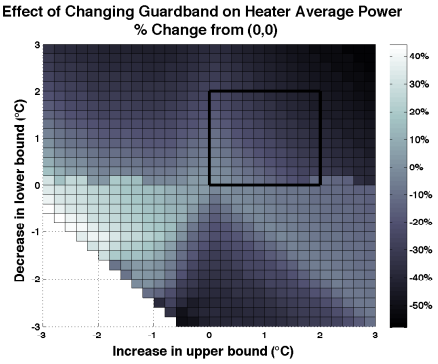

Fig. 5. The effect on average power consumption from changing the heater guardband constraints. The black square represents the region explored in this work (+/- 2°C). Within this region, power consumption varies by 47%, enabling significant responses to variations from renewable energy supplies. Note that a positive decrease in the lower guardband boundary reduces the lower guardband temperature.

That thermostatically-controlled loads are able to "walk" this graph – consuming comparatively more power at certain times while using less power at other times – allows them to follow source generation. This ability remains true for the fridge as well, and enables a range of flexibility in control strategies. In Figure 6, we show three different control scenarios of the house heater, with the rows representing temperature, power consumption, slack energy, and a two-day profile of wind energy from a wind farm in Minnesota. The gray area (lightly shaded) on the wind energy plots represents the maximum amount of "portfolio" or non-renewable energy drawn throughout the two-day period. The wind supply generation is the same for all three scenarios.

The first column represents an oblivious heater, which only considers its measured temperature when deciding if the compressor should be actuated. As such, it maintains a tight guardband and consistent slack energy profile. All of the wind plots have been scaled to provide 50% of the total energy needed to power this oblivious heater.

The second column ("supercool") represents a heater that allows the temperature to cool beyond its normal lower bound by 2°C when faced with a renewable energy shortage. The threshold for an energy shortage, represented by the maximum power consumption of the heater when operating, is indicated by the dashed line on the supply power graph in Figure 6. Thus, when wind energy is available, the heater operates in its standard tight guardband, consuming more energy.

The third column ("wide guardband") takes this concept further – this heater not only reduces power consumption when faced with a deficit of renewable energy, it also attempts to increase power when faced with a renewable energy surplus by running the heater for longer. In addition, to reduce the discretization of its response, this fridge scales the change in its guardband boundaries by the magnitude of the deficit or surplus of renewable energy. For example, in the late evening of the first day, wind energy far exceeds the threshold, the heater increases its guardband relatively more as compared to the early evening period, when wind energy barely exceeds the threshold. This change results in less energy saved than the "supercool" case because the proportional response is always less than or equal to 2°C.

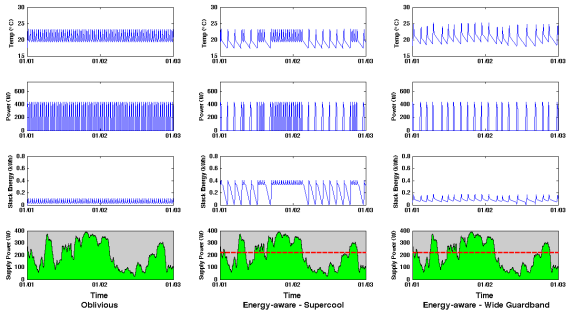

Fig. 6. Three scenarios of heater operation. The first column represents an "oblivious" heater that operates without any outside information, the second is a heater that allows the house to get cooler when faced with an energy deficit and the third is a heater that allows the house to get cooler when faced with an energy deficit as well as warmer when presented with an energy surplus.

What these scenarios show is that the heater can reduce the frequency of its cycles, and thus its energy consumption, when faced with an energy deficit. A natural follow-up question is whether house occupants are amenable to a wider guardband at certain times – this has been addressed widely in the building comfort and demand response literature. [5]

What is the magnitude of savings in these scenarios? Figure 7 compares the three; the first plot shows total energy consumption while the second considers the balance between renewable and portfolio energy. The ability to preferentially loosen guardband constraints saves significant energy – over 33% by reducing only the lower guardband boundary and over 50% while altering both the lower and upper boundaries, even with responses proportional to the energy deficit or surplus. The increase in energy savings from relaxing the lower guardband boundary is not surprising, but the large additional reduction from increasing the upper boundary is. This is because longer than standard actuation cycles (heating phases, in this case) ensure that the heater has a lower overall power consumption than the default scenario. We leave quantifying the limits of the potential reduction to future work.

Our final integration study examines the effects of aggregating the responses of a population of source-following loads. In Figure 8, we show the proportional change between renewable and portfolio energy as an aggregated population of loads increases. In this scenario, each fridge is initialized at a

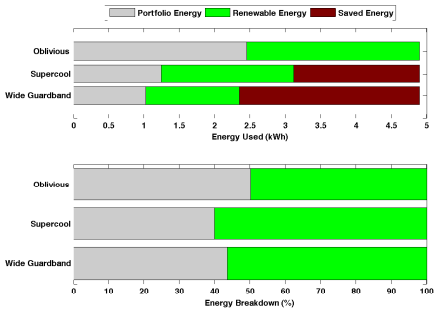

Fig. 7. The energy breakdown of the three heater scenarios. The top plot emphasizes the energy savings of increasing the guardband, while the bottom plot shows the improvement in the proportion of total energy that is renewable.

random phase with warming, cooling, and electrical behavior randomly selected from the normal distribution described in Section II-B1. Additionally, fridge responses are scaled to the magnitude of the energy deficits and surpluses, just as in the "wide guardband" heater described previously. Further – to more accurately represent actual behavior due to measurement error and local microclimatic effects – a small amount of randomness has been applied to the guardband boundaries, such that each time a boundary is approached, its value is increased or decreased by a random value within +/- 0.2°C. This small modification, while not capturing the entire variation among a large population of appliances, is beneficial in reducing the "herd effects" when a number of identical agents with identical control logic respond to the same stimulus. We believe that in practice, a population of fridges will in fact exhibit more variation than represented in this experiment. Also in this experiment, the wind energy supplied is scaled to satisfy 25% of the energy needed by the earlier described "oblivious" fridge. This restriction highlights the benefits of statistical multiplexing in a population.

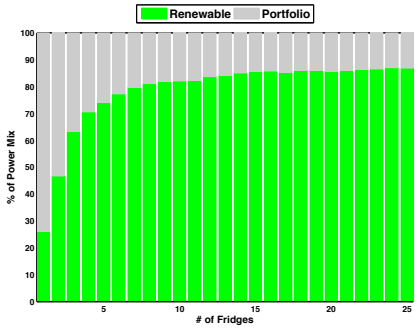

Fig. 8. The effects of population size on the proportion of total energy that is renewable. Variations of fridge periods and phases allows for cooperation without direct communication, making better use of renewable resources.

Looking at the results of the population study, the proportion of energy used by the fridges improves rapidly as the number of fridges increases, leveling off around 85%. With such limited wind energy supplied per fridge – with only one fridge, the wind supplies barely over 25% of the energy required for operation – there is significant improvement as each fridge is added. This is because fridges with slightly different guardbands and varied warming and cooling behavior operate at slightly different periods and phases, allowing individual fridges to use excess renewable energy not used by others in the population. As the population grows, the collection of power spikes resulting from the compression phases of each fridge blend into a flatter curve that begins to resemble the wind supply curve, reducing the overall difference between the consumption and the supply. We feel that this result coupled with the amplified variation among the actual population of fridges and similar gains from adapting other energy loads to be source-following forebears the potential for a substantial substitution of renewable energy in place of portfolio energy.

IV. Conclusion

As the fraction of the energy supply from renewable but unfortunately non-dispatchable sources like solar and wind increase in the coming decade, at least one of three things must happen to deal with the ensuing supply volatility: miraculous new energy storage technologies must be developed, renewable sources must be over-provisioned, or loads must adapt automatically to the waxing and waning of power. Recognizing that the first option requires some luck and the second option devalues renewable energy, we focus on third – adaptive loads.

In this work, we present a strategy for deep demand response of loads given a signal of energy availability. We have identified two broad classes of dispatchable appliances and constructed models that can be used to alter their control strategies. With these models, we create source-following loads that alter power consumption based on an actual wind energy trace. Our results show that not only can a significant proportion of energy be saved, but also that renewable energy consumption can be favored over other grid energy. Additionally, scaling to a larger population of source-following loads, an even larger proportion of the necessary energy can be provided by renewable sources. Considering the increasing velocity of the deployment of these non-dispatchable renewable energy sources as well as their high variability of generation, we believe that the type of deep demand response described in this work will be necessary to encourage the widespread growth of renewable energy sources while maintaining the balance between generators and loads required of the electricity grid.

Acknowledgment

This research was made with Government support under and awarded by DoD, Air Force Office of Scientific Research, National Defense Science and Engineering Graduate (NDSEG) Fellowship, 32 CFR 168a, along with support by the National Science Foundation under grant #CNS-0932209 (CPS-LoCal). Any opinions, findings and conclusions, or recommendations expressed in this material are those of the authors and do not necessarily reflect the views of the listed funding agencies.

References

[1] "Database of State Incentives for Renewables and Efficiency," http://www.dsireusa.org.
[2] "State of California Executive Order S-21-09," http://gov.ca.gov/executive-order/13269.
[3] "Automated Demand Response Program," http://www.auto-dr.com/.
[4] "Appliance Energy Use Data Repository," http://minotaur.lbl.gov/aeud/.
[5] T. Hoyt, K. H. Lee, H. Zhang, E. Arens, and T. Webster, "Energy savings from extended air temperature setpoints and reductions in room air mixing," in *Proceedings of the International Conference on Environmental Ergonomics 2009*, 2009.